Data-Driven and Minimal-Type Compartmental Insulin-Glucose Models: Theory and Applications

Georgios D. Mitsis and Vasilis Z. Marmarelis

Abstract This chapter initially presents the results of a computational study that compares simulated compartmental and Volterra models of the dynamic effects of insulin on blood glucose concentration in humans. In this context, we employ the general class of Volterra-type models that are estimated from input-output data, and the widely used "minimal model" as well as an augmented form of it, which incorporates the effect of insulin secretion by the pancreas. We demonstrate both the equivalence between the two approaches analytically and the feasibility of obtaining accurate Volterra models from insulin-glucose data generated from the compartmental models. We also present results from applying the proposed approach to quantifying the dynamic interactions between spontaneous insulin and glucose fluctuations in a fasting dog. The results corroborate the proposition that it may be feasible to obtain data-driven models in a more general and realistic operating context, without resorting to the restrictive prior assumptions and simplifications regarding model structure and/or experimental protocols (e.g. glucose tolerance tests) that are necessary for the compartmental models proposed previously. These prior assumptions may lead to results that are improperly constrained or biased by preconceived (and possibly erroneous) notions—a risk that is avoided when we let the data guide the inductive selection of the appropriate model.

G. D. Mitsis (✉)
Department of Electrical and Computer Engineering, University of Cyprus,
P.O. Box 20537 Kallipoleos 75 1678 Nicosia, Cyprus
e-mail: gmitsis@ucy.ac.cy

G. D. Mitsis
Department of Bioengineering, McGill University, P.O. Box 20537
817 Sherbrooke St. W., Macdonald Engineering Building, Montreal,
QC H3A 0C3, Canada

V. Z. Marmarelis
Department of Biomedical Engineering, University of Southern California,
1042 Downey Way, Denney Research Center 140,
Los Angeles 90089 CA, USA
e-mail: vzm@bmsr.usc.edu

V. Marmarelis and G. Mitsis (eds.), *Data-driven Modeling for Diabetes*,
Lecture Notes in Bioengineering, DOI: 10.1007/978-3-642-54464-4_1,

1 Introduction

Diabetes mellitus represents an alarming threat to public health with rising trends and severity in recent years worldwide and is characterized by multiple and often not readily observable clinical effects [15]. Hence, there is urgent need for improved diagnostic methods that provide more precise clinical assessments and sensitive detection of symptoms at earlier stages of the disease [33]. This critical task may be facilitated (or enabled) by the utilization of advanced mathematical models that reliably describe the dynamic interrelationships among key physiological variables implicated in the underlying physiology (i.e. blood glucose concentration and various hormones such as insulin, glucagon, epinephrine, norepinephrine, cortisol etc.) under a variety of metabolic and behavioral conditions (e.g. pre-/post-prandial, exercise/rest, stress/relaxation). Such models would not only provide a powerful diagnostic tool, but may also enable long-term glucose regulation in diabetics through closed-loop model-reference control using frequent insulin micro-infusions administered by implanted programmable micro-pumps. This may prevent the onset of the pathologies caused by elevated blood glucose over prolonged periods in diabetic patients [15].

The primary effect on blood glucose is exercised by insulin and most efforts to date have focused on the study of this causal relationship. Prolonged hyperglycemia is usually caused by defects in insulin secretion by the pancreatic beta cells or in the efficiency of insulin-facilitated glucose uptake by the cells. The exact quantitative nature of the dependence between blood glucose concentration and the action of the other hormones mentioned above, or factors such as diet, endocrine cycles, exercise, stress etc. remains largely unknown—primarily because of lack of appropriate data although the qualitative effect has been established. Thus, the aggregate effect of all these other factors for modeling purposes is viewed as random "disturbances", additive to the blood glucose level.

Starting from the initial work of Bolie [7] and Ackerman [1], most modeling studies of the causal relationship between insulin and glucose (as the "input" and "output" of a system representing this relationship) have relied on the concept of compartmental modeling [9]. In this context, the minimal model (MM) of glucose disappearance, combined with the intravenous glucose tolerance test, has been the most widely used method to study whole body glucose metabolism in vivo [3]. The MM postulates that insulin acts from a remote compartment and affects glucose utilization, in addition to the insulin-independent utilization that depends on the glucose level *per se*. These insulin-dependent and insulin-independent effects on glucose utilization/kinetics are combined in a single compartment. Certain parameters of the MM (i.e., insulin sensitivity SI and glucose effectiveness SG) have been shown to be of clinical importance and can be estimated from IVGTT data, using nonlinear least-squares methods [4, 34] or, more recently, Bayesian estimation techniques [22, 23].

The accuracy of the estimates obtained from the MM has been questioned because of the single-compartment assumption [10, 16, 34], and two-compartment

models for glucose kinetics have been proposed [8,11]. Moreover, more complex models that aim to capture the complexity of the underlying physiology under more general operating conditions have been also proposed [13, 14, 38]. However, models of this type cannot be identified from standard clinical tests and they require the design of specialized experimental protocols. For instance, the model proposed in [14] includes 12 differential equations and 35 parameters, and a specialized triple-tracer experiment was designed in order to identify its parameters in 204 healthy individuals and 58 pre-diabetic/diabetic patients [14]. Other modeling approaches that have been explored—in the context of glucose control—include artificial neural networks [43], probabilistic models [2] and linear/nonlinear impulse response and Volterra models [18, 27, 35]. In addition to modeling insulin-glucose interactions, attempts have been made to take into account the influence of additional relevant physiological signals, such as glucagon [13, 26] and free fatty acids [37].

Most of the aforementioned compartmental models rely on *a priori* assumptions and simplifications regarding the underlying physiological mechanisms and their primary aim is often to extract clinically important parameters in conjunction with specific experimental protocols (e.g., the IVGTT). Therefore, their ability to quantify glucose metabolism under actual, more general operating conditions remains limited. On the other hand, recent technological advances in the development of reliable continuous glucose sensors and insulin micro-pumps [6, 19] have provided time-series data that enable the application of data-driven modeling approaches. These approaches offer new opportunities towards the goal of obtaining reliable models of the insulin-glucose interrelationships in a more general context. Using spontaneous or externally infused insulin and glucose data, one can obtain data-driven models that are not constrained by *a priori* assumptions regarding their structure.

In addition to the effects of external insulin or glucose stimuli, the interactions between spontaneous fluctuations of plasma glucose and insulin are of great interest. The precise characteristics of pulsatile insulin secretion patterns influence blood glucose regulation and are altered in Type II diabetes [24, 36]. Furthermore, insulin secretion is regulated in vivo by plasma glucose oscillations over various time scales (from rapid to ultradian) and changes in this relation may be potentially useful as an early marker of Type II diabetes development [36, 40].

Therefore, the purpose of the present chapter is twofold: First, we examine the relation between existing compartmental (differential equation) and Volterra-type models, both analytically and computationally. The results demonstrate the feasibility of obtaining Volterra models of insulin-glucose dynamics that are equivalent to widely accepted compartmental models, using data-records that are practically obtainable. They also illustrate the physiological interpretation of nonlinear Volterra models by providing direct links to a well-known parametric model with parameters of clinical significance. Since the Volterra approach does not require prior assumptions about model structure, it can provide the effective means for obtaining accurate data-true, patient-specific and time-adaptive models in a clinical context. Second, we showcase the application of the proposed data-

driven approach to modeling the dynamic interrelationships between spontaneous variations of plasma insulin and glucose in fasting dogs in the closed-loop context of the problem. Specifically, we examine both causal directions of the loop—i.e. considering first the insulin as input and the glucose as output, and vice versa. The resulting Principal Dynamic Modes (PDM) models are equivalent to Volterra models and have a modular form that facilitates physiological interpretation. The analysis of the experimental data yields PDM models that are comprised of two parallel branches in each causal direction, describing the primary physiological mechanisms of slow and fast dynamic interactions between variations of plasma insulin and glucose for each causal direction. Spectral analysis of the resulting insulin and glucose residuals (representing internal secretions and systemic disturbances) indicate the presence of oscillatory spontaneous variations of insulin and glucose at preferred frequencies in agreement to previous reported observations. Overall, our results demonstrate the potential of the proposed black-box modeling approach to advance our quantitative understanding of this system.

2 Insulin-Glucose Models

The present study concerns compartmental and Volterra-type nonlinear dynamic models; among compartmental models, we select the minimal model of glucose disappearance (MM), as well as an augmented version of it (AMM), which incorporates an insulin secretion equation. The structure and parameter values of these models are taken from the literature [3, 4, 20, 25, 41, 45]. The equivalent Volterra models [30] are estimated using simulated input–output data from the compartmental models in Sect. 3.

2.1 The Minimal Model of Glucose Disappearance

The MM of glucose disappearance is described by the following two differential equations [3], which describe the nonlinear dynamics of the insulin-to-glucose relationship during an IVGTT:

$$\frac{dg(t)}{dt} = -p_1 g(t) - x(t)[g(t) + g_b] \tag{1}$$

$$\frac{dg(t)}{dt} = -p_2 x(t) + p_3 i(t) \tag{2}$$

where $g(t)$ is the deviation of glucose plasma concentration from its basal value g_b (in mg/dl), $x(t)$ is the internal variable of insulin action (in min^{-1}), $i(t)$ is the deviation of insulin plasma concentration from its basal value i_b (in μU/ml), p_1 and

p_2 are parameters describing the kinetics of glucose and insulin action respectively (in min^{-1}) and p_3 is a parameter (in $\text{min}^{-2}\text{ml}/\mu\text{U}$) that affects insulin sensitivity SI (see below). The initial conditions for the simulations are: $g(0) = 0$ and $x(0) = 0$ (i.e. we assume that we start at basal conditions—which is a reasonable assumption in the context of simulating the model for situations where the initial "transient" phase can be ignored). Note that the MM is nonlinear, due to the presence of the bilinear term between the internal variable $x(t)$ representing insulin action and the variable $g(t) + g_b$ representing the plasma glucose concentration in the first equation. This bilinear term describes the modulation of the effective kinetic constant of the glucose utilization by insulin action (i.e. insulin concentration increases cause faster disappearance of blood glucose).

The physiological interpretation of the MM parameters can be made in terms of insulin-dependent and insulin-independent processes that enhance glucose uptake and suppress net glucose output. The parameter p_1, termed "glucose effectiveness" SG, represents the insulin-independent effect, while the insulin-dependent effect is represented by the ratio p_3/p_2 (in $\text{min}^{-1}/\mu\text{Uml}^{-1}$) and is termed "insulin sensitivity" SI. The values of SG and SI are typically estimated from IVGTT data and the MM has proven to be successful in a clinical context, requiring a relatively simple test procedure [5]. Nonetheless, the accuracy and physiological interpretation of the MM parameter estimates has been questioned because of the use of a single compartment for glucose kinetics [10, 11].

The MM, as formulated in Eqs. (1) and (2), does not include an equation describing the secretion of insulin from pancreatic beta cells in response to an elevation in blood glucose concentration, i.e., it is an open-loop model, which may be used along with properly designed experimental protocols (IVGTT) for parameter estimation. However, the actual glucose metabolism process is a closed-loop system, except in conditions of severe Type I diabetes where the pancreatic beta cells are considered totally inactive. In order to account for this, an insulin secretion equation may be included, as described below (closed loop MM or AMM). Limitations of the MM (and the AMM) include the absence of an explicit glucogenic component reflecting production of new glucose by the liver in response to elevated plasma insulin and/or glucose (such as the model presented in [26]) and the associated glucagon secretion process (from the alpha cells of the pancreas) among others. The aggregate effect of these processes, as well as the effect of other factors (free fatty acids, epinephrine etc.), can be incorporated by "disturbance" terms that are added to the glucose rate and insulin action equations.

2.2 *Closed-Loop Compartmental Model: The Augmented Minimal Model*

The closed-loop nature of insulin-glucose interactions requires the incorporation of an additional equation describing the insulin secretion dynamics by the pancreatic beta cells. Of several equations that have been proposed [4, 39, 41, 42, 45], we

select one that utilizes a threshold function, similar to the one reported in [42]. The resulting closed-loop model becomes:

$$\frac{dg(t)}{dt} = -p_1 g(t) - x(t)[g(t) + g_b] \tag{3}$$

$$\frac{dx(t)}{dt} = -p_2 x(t) + p_3[i(t) + r(t)] \tag{4}$$

$$\frac{dr(t)}{dt} = -ar(t) + \beta T_h[g(t)] \tag{5}$$

where $r(t)$ is the secreted insulin by the pancreatic beta cells in response to an elevation in plasma glucose concentration and $i(t)$ correspond to insulin concentration changes due to externally administered insulin. The secretion is triggered by elevated plasma glucose concentrations according to the threshold function $T_h[g(t)]$ defined as:

$$T_h[g(t)] = \begin{cases} g(t) - \theta & g(t) \geq \theta \\ 0 & otherwise \end{cases} \tag{6}$$

where θ corresponds to the glucose concentration value above which insulin is secreted. The dynamics of this triggered secretion process and the kinetics of the secreted insulin are described (in first approximation) by the kinetic constant a (in min^{-1}) in Eq. (5). The parameter β (in $\mu\text{U min}^{-1}$/ml per mg/dl) determines the rate of insulin secretion (i.e. the strength of the feedback pathway). Note that some alternative similar models [4, 41] of insulin secretion include a time-varying term that multiples the last term of Eq. (5) with t. This is based on the hypothesis that the rate of insulin secretion in response to hyperglycemia increases linearly with time. However, this term may not admit a steady-state solution but instead result in unbounded state variable values for physiologically reasonable values of the model parameters. This is not plausible; therefore, it should be taken into account when constructing models that are intended to be physiologically realistic, as discussed in more detail in the chapter by Panunzi and de Gaetano in the present volume.

2.3 Volterra-Type Models

The Volterra-Wiener framework has been employed extensively for modeling nonlinear physiological systems [30]. In this context, the input-output dynamic relationship of a causal, nonlinear system of order Q and memory M is described by the Volterra functional expansion:

$$g(t) = \sum_{n=0}^{Q} \int_0^M \dots \int_O^M k_n(\tau_1, \dots, \tau_n) i(t - \tau_1) \dots i(t - \tau_n) d\tau_1 \dots d\tau_n \tag{7}$$

The Volterra model can be formulated in discrete-time as follows:

$$g(t) = \sum_{n=0}^{Q} \sum_{\tau_1=0}^{M} \dots \sum_{\tau_n=0}^{M} k_n(\tau_1, \dots, \tau_n) i(t-\tau_1) \dots i(t-\tau_n) \tag{8}$$

In both the above models (Eqs. 7 and 8), $i(t)$ and $g(t)$ are the input and output of the system at time t (deviations of plasma insulin and glucose concentrations from their basal values, respectively). The unknown quantities of the Volterra model that are estimated from the input-output data are the Volterra kernels $k_n(\tau_1,\dots, \tau_n)$. The first-order kernel ($n = 1$) is the linear component of the system dynamics, while the higher order kernels ($n > 1$) form a hierarchy of the nonlinear dynamics of the system. The highest order Q defines the nonlinear order of the system. Many physiological systems can be described adequately by Volterra models of relatively low order (second or third) [30]. The Volterra-Wiener approach is well-suited to the complexity of physiological systems since it yields data-true models, without requiring a priori assumptions about system structure.

Among various methods that have been developed for the estimation of the discrete-time Volterra kernels (Eq. 8), a Volterra-equivalent network in the form of the Laguerre-Volterra Network (LVN) is selected because it has been proven to be an efficient approach that yields accurate representations of high-order systems in the presence of noise using short input-output records [31]. The LVN model consists of an input layer of a Laguerre filter-bank and of a hidden layer with K hidden units with polynomial activation functions (Fig. 1) [31]. At each discrete time t, the input signal $i(t)$ (insulin) is convolved with the Laguerre filter-bank and weighted sums of the filter-bank outputs V_j (where $v_j = i * b_j$, * denotes convolution and b_j is the j-th order discrete-time Laguerre function) are transformed by the hidden units through polynomial transformations.

The model output $g(t)$ (glucose) is formed as the summation of the hidden unit outputs z_k and a constant corresponding to the glucose basal value g_b:

$$u_k(t) = \sum_{j=0}^{L-1} w_{k,j} v_j(t) \tag{9}$$

$$g(t) = \sum_{k=1}^{K} z_k(t) + g_b = \sum_{k=1}^{K} \sum_{n=1}^{Q} c_{n,k} u_k^n(t) + g_b \tag{10}$$

where L is the number of functions in the filter bank and $w_{k,j}$ and $c_{n,k}$ are the weighting and polynomial coefficients respectively. The insulin and glucose time-series are used to train the LVN model parameters ($w_{k,j}$, $c_{n,k}$ and the Laguerre parameter which determines the Laguerre functions dynamic properties) with a gradient-descent algorithm, as described in [31].

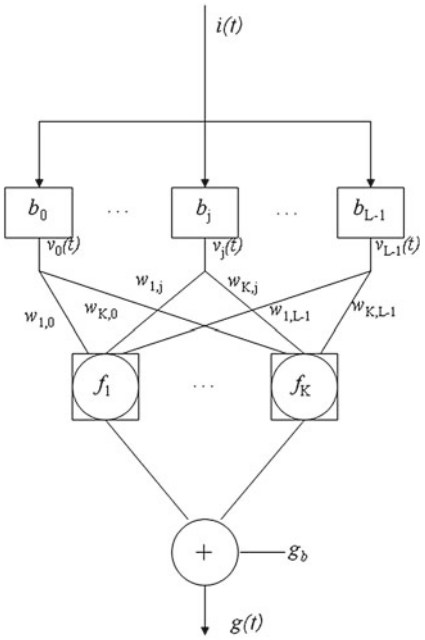

Fig. 1 The Laguerre-Volterra network. The system input $i(t)$ is convolved with a Laguerre filter bank with impulse responses b_j, the outputs of which ($v_j(n)$) are fed into a layer of K hidden units with polynomial activation functions f_K that produce the system output $g(t)$

The equivalent Volterra kernels are then obtained in terms of the LVN parameters as:

$$k_n(\tau_1,\ldots,\tau_n) = \sum_{k=1}^{K} c_{n,k} \sum_{j_1=0}^{L-1} \ldots \sum_{j_n=0}^{L-1} w_{k,j_1} \ldots w_{k,j_n} b_{j_1}(\tau_1) \ldots b_{j_n}(\tau_n) \qquad (11)$$

The structural parameters of the LVN model (L, K, Q) are selected on the basis of the normalized mean-square error (NMSE) of the output prediction achieved by the model, defined as the sum of squares of the model residuals divided by the sum of squares of the demeaned true output. The statistical significance of the NMSE reduction achieved for model structures of increased order/complexity is assessed by comparing the percentage NMSE reduction with the alpha-percentile value of a chi-square distribution with p degrees of freedom (p is the increase of the number of free parameters in the more complex model) at a significance level alpha, typically set at 0.05.

The LVN representation is equivalent to a variant of the general Wiener-Bose model termed the Principal Dynamic Mode (PDM) model. The PDM model consists of a set of parallel branches, each one of which is the cascade of a linear dynamic filter (PDM) followed by a static nonlinearity [29, 30]. Each of the K hidden units of the LVN corresponds to a separate branch and defines the respective PDM $p_k(t)$ and polynomial nonlinearity $f_k(.)$. This leads to model representations that allow physiological interpretation, since the resulting number of branches is typically low

in practice. According to the PDM model form, the insulin input signal is convolved with each of the PDMs $p_k(t)$, where $k = 1, \ldots, K$ and $p_k(t) = \sum_{j=0}^{L-1} w_{k,j} b_j(t)$, and the PDM outputs u_k are subsequently transformed by the respective polynomial nonlinearities $f_k(.)$ to produce the model-predicted blood glucose output (the asterisk denotes convolution) [30]:

$$\begin{aligned} g(t) &= g_b + f_1[u_1(t)] + \ldots + f_K[u_K(t)] \\ &= g_b + f_1[p_1(t) * i(t)] + \ldots + f_K[p_K(t) * i(t)] \end{aligned} \tag{12}$$

Therefore, once an LVN model is trained based on input-output data, the PDMs and their associated nonlinearities can be readily obtained using the final (trained) values of the LVN parameters, i.e., weights $w_{k,j}$, polynomial coefficients $c_{n,k}$ and Laguerre parameter α. For more details, the reader is referred to [32] (Chap. 2).

3 Comparison Between Compartmental and Volterra Models

3.1 Generalized Harmonic Balance Method

In order to examine the mathematical relationship between the aforementioned compartmental and Volterra models, we employ the generalized harmonic balance method to derive analytical relations between the two model forms, as outlined below for the second-order case of the nonparametric model [28]. This procedure can be extended to any order of interest.

By setting the input $i(t)$ equal to 0, e^{st} and $e^{s_1 t} + e^{s_2 t}$ in the general Volterra model of Eq. (7) successively, the output $g(t)$ becomes equal to k_0, $k_0 + e^{st}K_1(s) + e^{2st}K_2(s, s) + \ldots$ and $k_0 + e^{s_1 t}K_1(s_1) + e^{s_2 t}K_1(s_2) + e^{s_1 t + s_2 t}K_2(s_1, s_2) + \cdots$ where $K_1(s)$ and $K_2(s_1, s_2)$ are the Laplace transforms of $k_1(\tau)$ and $k_2(\tau_1, \tau_2)$ respectively. If we substitute these three input-output pairs into the differential equations of the compartmental models (Eqs. 1 and 2) for the open-loop model and (3–5) for the closed-loop model) and equate the coefficients of the resulting exponentials of the same kind, we can obtain analytical expressions for k_0, $K_1(s)$ and $K_2(s_1, s_2)$, in terms of the parameters of the respective compartmental model.

To define the computational equivalence between the two model forms, we simulate the compartmental models with broadband input (insulin) data and we then estimate the kernels of the equivalent Volterra model, from the simulated input- output data. The accuracy of the estimated first and second-order Volterra kernels is assessed by comparison with the exact kernels of the equivalent Volterra model that is derived in analytical form from the differential equations of the compartmental models. The accuracy and robustness of the kernel estimates is evaluated under measurement noise conditions, in order to assess the performance of the Volterra approach.

3.2 Analytical Expressions of the Volterra Kernels of the Compartmental Model: Open-Loop Case

The bilinear term between insulin action and glucose concentration in Eq. (1) of the MM gives rise to an equivalent Volterra model of infinite order. However, for parameter values within the physiological range, a second-order Volterra model offers an adequate approximation for all practical purposes. Considering the insulin and glucose deviations from the respective basal values $i(t)$ and $g(t)$ as the input and the output respectively, we can derive analytically the Volterra kernels of the open-loop MM by applying the procedure outlined in Sect. 3.1 to the integro-differential equation:

$$\dot{g}(t) + p_1 g(t) + p_3 \int_0^\infty exp(-p_2\tau) i(t-\tau) d\tau = -g_b p_3 \int_0^\infty exp(-p_2\tau) i(t-\tau) d\tau \tag{13}$$

The above equation is derived from the MM by substituting the convolutional solution of Eq. (2):

$$x(t) = p_3 \int_0^\infty exp(-p_2\tau) i(t-\tau) d\tau \tag{14}$$

into Eq. (1). Upon application of this method, we derive the following analytical expressions in the Laplace domain for the first- and second-order Volterra kernels of the MM ($k_0 = 0$):

$$K_1(s) = p_3 g_b \frac{1}{(s+p_1)(s+p_2)} \tag{15}$$

$$K_2(s_1, s_2) = \frac{p_3^2 g_b}{2} \frac{1}{(s_1+p_1)(s_1+p_2)} \frac{1}{(s_2+p_1)(s_2+p_2)} \left[1 + \frac{p_2}{s_1+s_2+p_1}\right]. \tag{16}$$

The MM has, in principle, Volterra kernels of any order. However, it can be shown that the magnitude of the n-th order kernel is proportional to the n-th power of p_3 and, subsequently, an adequate Volterra model may only include the first two kernels (since the value of p_3 is on the order of 10^{-5}–10^{-4}). The resulting expressions for the first and second order kernels in the time domain are given in Eqs. (17) and (18) respectively:

$$k_1(\tau) = -g_b \frac{p_3}{p_2 - p_1} [\exp(-p_2\tau_1) - \exp(-p_2\tau)] \tag{17}$$

$$k_2(\tau_1,\tau_2) = \frac{p_3^2 g_b}{2(p_2-p_1)^2}\Bigg[[\exp(-p_1\tau_1)-\exp(-p_2\tau_1)][\exp(-p_1\tau_2)-\exp(-p_2\tau_2)] + p_2\Bigg[\Bigg[\frac{1}{p_1}\exp[-p_1(\tau_1+\tau_2)].[\exp(p_1\min(\tau_1,\tau_2)-1)]\Bigg] - \frac{1}{p_2}\exp[(-p_1\tau_1-p_2\tau_2)+\exp(-p_1\tau_2-p_2\tau_1)](\exp[p_2\min(\tau_1,\tau_2)]-1) + \frac{\exp(-p_2(\tau_1-\tau_2))}{2p_2-p_1}(\exp[(2p_2-p_1)\min(\tau_1,\tau_2)]-1)\Bigg]\Bigg] \tag{18}$$

These first and second-order Volterra kernels are plotted in Fig. 2 (top panel) for typical MM parameter values within the physiological range [25, 34]: g_b= 80 mg/dl, p_1= S_G = 0.02 min^{-1}, p_2 = 0.028 min^{-1} and p_3= 10^{-4} min^{-2}ml/μU, which yield S_1= 0.0036 min^{-1}/μU ml^{-1}. Since the specific parameter values define the MM description of insulin-glucose dynamics, they also define the form of the equivalent Volterra kernels. The form of the first-order kernel in Fig. 2 (top left panel) indicates that an 10 μU/ml insulin concentration increase will cause a first-order drop in plasma glucose concentration that will reach a minimum of about −1.2 mg/dl about 36 min later, rising after that to half the drop in about 1 h and relaxing back to the basal value about 4 h after the minimum. The positive values of the second-order Volterra kernel indicate that the actual glucose drop caused by the insulin infusion will be slightly less than the first-order prediction (sublinear response). For instance, an insulin concentration increase of 100 μU/ml will not cause a maximum glucose drop of 12 mg/dl (as predicted by its equivalent first-order kernel) but a drop of about 10.5 mg/dl due to the antagonistic second-order kernel contribution.

Changes in these parameter values affect the form and the values of the kernels in the precise manner described by Eqs. (17) and (18). The effects of changes in the two MM parameters p_1 and p_2 on the equivalent first-order kernel are illustrated in Fig. 2 (bottom panels) for a range of physiological values (p_1 between 0.01 and 0.04 min^{-1} and p_2 between 0.02 and 0.05 min^{-1} [34], keeping $p_3 = 10^{-4}$ min^{-2} ml/μU constant). Note that changes in p_3 simply scale the first-order kernel according to Eq. (17) and do not alter its form (proportional dependence)—nor do they alter the form of the second-order kernel (they scale it quadratically). A direct sense of the effects of parameter changes is obtained by the waveforms of Fig. 2: for instance, as $p_1(S_G)$ increases, the maximum drop of the first-order kernel becomes smaller and its dynamics (i.e. the drop to the minimum and the return to basal value) become faster. Similar effects are observed when p_2 increases (or S_I decreases).

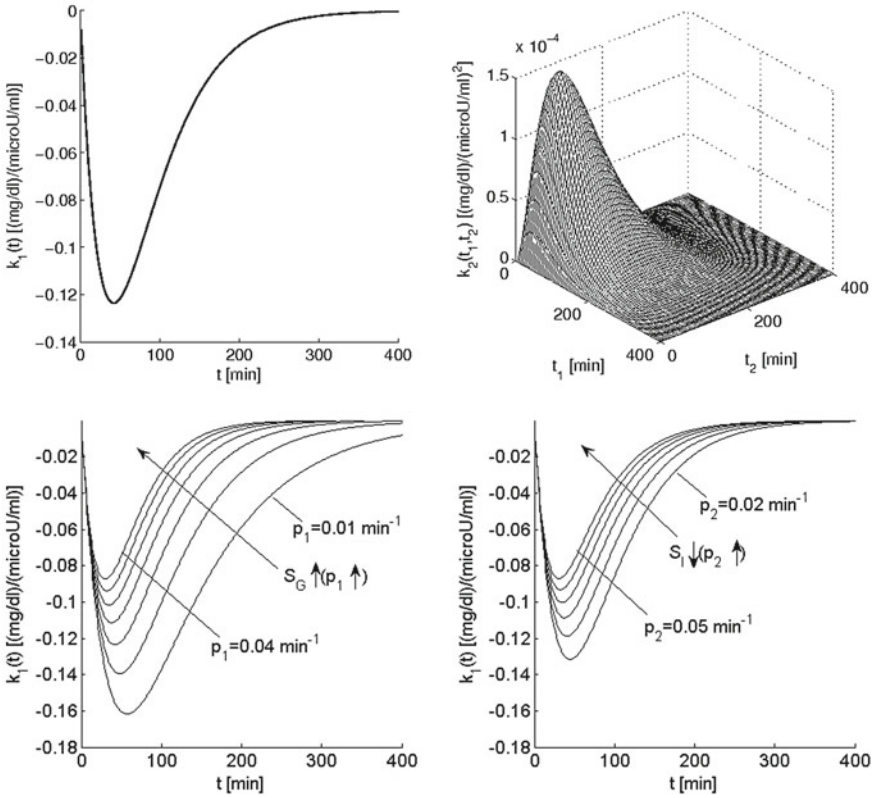

Fig. 2 *Top panel* The first-order (*left*) and second-order (*right*) Volterra kernels of the minimal model for typical values of its parameters within the physiological range ($S_G = 0.02\ \text{min}^{-1}$ and $S_I = 0.0036\ \text{min}^{-1}/\mu\text{U ml}^{-1}$). *Bottom panel* Effect of the two key parameters p_1 and p_2 of the open-loop MM on the form of the equivalent first-order kernel. Note that the glucose effectiveness S_G is equal to p_1 and the insulin sensitivity S_I is inversely proportional to p_2 (and proportional to p_3). These plots offer a visual understanding of the effects of changes in these parameters (p_1 between 0.01 and 0.04 min^{-1}, p_2 between 0.02 and 0.05 min^{-1}) on the first-order insulin-glucose dynamics (see text)

3.3 Analytical Expressions of the Volterra Kernels of the Compartmental Model: Closed-Loop Case

To derive the analytical expressions of the kernels in the closed-loop case, we approximate the threshold function of Eq. (6) with a polynomial as indicated below, assuming that θ is equal to zero (i.e. insulin secretion is triggered when the glucose concentration rises above its basal value):

$$\beta T_h[g(t)] \approx \beta_1 g(t) + \beta_1 g^2(t) + \ldots \tag{19}$$

where $g(t)$ is the deviation of glucose plasma concentration from its basal value. Equation (19) provides an accurate representation of (6) within a desired dynamic range for glucose values $g(t)$ (Weierstrass theorem), whereby the coefficients β_i can be estimated in a mean-square sense. However, note that the subsequent analysis is valid for any values of these coefficients. Equation (5) can be rewritten as:

$$\frac{dr(t)}{dt} = -ar(t) + \beta_1 g(t) + \beta_2 g^2(t) + \ldots \tag{20}$$

The solution of Eq. (20) is given by:

$$r(t) = \beta_1 f(t) * g(t) + \beta_2 f(t) * g^2(t) + \ldots \tag{21}$$

where the asterisk denotes convolution and $f(t) = e^{-at}u(t)$. Also, from Eq. (4) we have

$$\frac{dx(t)}{dt} = -p_3 h(t) * [i(t) + r(t)] \tag{22}$$

where $h(t) = e^{-p_2 t}u(t)$. Then, Eq. (3) becomes:

$$\frac{dg(t)}{dt} + p_1 g(t) = -p_3 g(t)\big[h(t) * i(t) + \beta_1 h(t) * f(t) * g(t) + \beta_2 h(t) * f(t) * g^2(t) + \ldots\big]. \tag{23}$$

The above equation can be used to obtain the equivalent Volterra kernels of the closed-loop model, following the procedure outlined before for the open-loop model. The resulting expressions for the first-order and the second-order kernels in the Laplace domain are given by Eqs. (24) and (25) respectively ($k_0 = 0$):

$$K_1(s) = -p_3 g_b \frac{H(s)}{(s + p_1 + p_3 g_b \beta_1 F(s) H(s))} \tag{24}$$

$$\begin{aligned} K_2(s_1, s_2) = & -p_3[(\beta_1 + \beta_2)] g_b \frac{H(s_1 + s_2) F(s_1 + s_2) K_1(s_1) K_1(s_2)}{s_1 + s_2 + p_1 + p_3 g_b \beta_1 H(s_1 + s_2) F(s_1 + s_2)} \\ & + \frac{1}{2} \frac{H(s_1) K_1(s_2) H(s_2) K_1(s_1)}{s_1 + s_2 + p_1 + p_3 g_b \beta_1 H(s_1 + s_2) F(s_1 + s_2)} \end{aligned} \tag{25}$$

where $F(s)$, $H(s)$ are the Laplace transforms of $f(t)$, $h(t)$ respectively, i.e. $F(s) = \frac{1}{s+a}$, $H(s) = \frac{1}{s+p_2}$.

The above relations were inverted numerically to yield the time-domain expressions for the first-order kernel, which are shown in Fig. 3 for the following parameter values: a varying between 0.1 and 0.3 min^{-1} with β remaining constant at 0.05 $\mu\text{U-min}^{-2}$/ml per mg/dl (left panel) and β varying between 0.0001 and 0.1

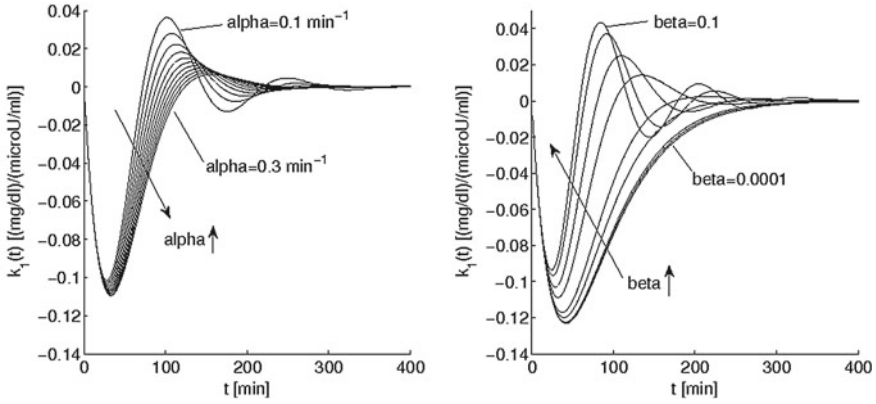

Fig. 3 The first-order kernels of the AMM for a varying between 0.1 and 0.3 min^{-1} with constant $\beta = 0.05$ (*left panel*) and for β varying between 0.0001 and 0.1 μU-min^{-2}/ml per mg/dl with constant $a = 0.13$ min^{-1} (*right panel*)

μU-min^{-2}/ml per mg/dl with a remaining constant at 0.13 min^{-1} (right panel). The nominal value of a (0.13 min^{-1}) was taken from [45], while the value of β was set at 0.05 μU-min^{-2}/ml, since the value reported in [45] (0.0054) resulted in negligible effects of endogenous insulin secretion for the stimuli used in this study. The decrease of a (slower insulin secretion dynamics) and increase of β (stronger feedback) affect the AMM first-order kernel waveform similarly—i.e., they result in faster dynamics with a small decrease of the negative peak value and the appearance of an overshoot which is characteristic of closed-loop systems.

3.4 Simulation Results: Open-Loop Model

In order to demonstrate the feasibility of estimating the Volterra kernels of the open-loop MM directly from input-output measurements, we simulate it by numerical integration of Eqs. (1) and (2) for the following values of MM parameters: $p_1 = 0.020$ min^{-1}, $p_2 = 0.028$ min^{-1}, $p_3 = 10^{-4}$ min^{-2} ml/μU, $g_b = 80$ mg/dl that are around the middle of the physiological ranges reported in the literature [4, 34]. The input signal for this simulation is a zero-mean Gaussian white noise (GWN) sequence of insulin time-series (i.e. independent samples every 5 min), with a standard deviation of 4 μU/ml, which may be viewed as spontaneous fluctuations around its basal value or arising from step-wise continuous infusions of insulin at random levels, changed every 5 min, superimposed on a constant (positive) baseline infusion. Due to the low-pass dynamic characteristics of the model, one sample every 5 min is sufficient for representing the input-output data. An input-output record of 144 sample points (i.e., 12 h long) is used to perform the training of the LVN and the estimation of the kernels of the equivalent Volterra model.

Table 1 Output prediction NMSEs for various LVN model structures and values of p_3, GWN input (open-loop case)

L	$p_3 = 5 \cdot 10^{-5}$		$p_3 = 5 \cdot 10^{-4}$		$p_3 = 5 \cdot 10^{-4}$	
	$\text{min}^{-2}\text{ml}/\mu\text{U}$		$\text{min}^{-2}\text{ml}/\mu\text{U}$		$\text{min}^{-2}\text{ml}/\mu\text{U}$	
	Linear NMSE	Nonlinear NMSE	Linear NMSE	Nonlinear NMSE	Linear NMSE	Nonlinear NMSE
2	13.55	8.97	16.24	15.46	22.42	4.89
3	0.39	0.32	0.68	0.30	23.23	1.13
4	4.62	4.85	3.33	3.63	23.88	3.73
5	0.17	0.14	0.40	0.09	21.35	0.61
6	0.22	0.31	0.39	0.17	21.82	0.61

The value of p_3 determines the relative contribution of the nonlinear terms: note that for $p_3 = 5 \cdot 10^{-5}$ min^{-2} ml/μU the NMSE reduction achieved by nonlinear models is marginal, while for $p_3 = 5 \cdot 10^{-4}$ min^{-2} ml/μU it is over 20 %. Using $L > 5$ does not improve model performance further

In order to illustrate model structure selection, we show the obtained NMSEs for various values of L, as well as for linear ($Q = 1$) and nonlinear ($Q = 2$) models for three different values of p_3, which determines the strength of the MM nonlinearity, in Table 1. For $p_3 = 5 \cdot 10^{-5}$ $\text{min}^{-2}\text{ml}/\mu\text{U}$ the model is weakly nonlinear, whereas for $p_3 = 5 \cdot 10^{-4}$ $\text{min}^{-2}\text{ml}/\mu\text{U}$ the NMSE reduction achieved for $Q = 2$ is over 20 %. The contribution of the n-th order Volterra term is proportional to the n-th power of the product of parameter p_3 with the power level of the input (i.e., this contribution increases for larger insulin variations); however, for the range of values examined, a second-order model is found to be sufficient. Also, using $L > 5$ reduces the NMSE minimally in all cases. Therefore, we select a second-order LVN with one hidden unit and five Laguerre functions (i.e., $L = 5$, $K = 1$, $Q = 2$) for the estimation of the equivalent Volterra model, with the resulting output prediction NMSE being 0.09 % ($p_3 = 10^{-4}$ $\text{min}^{-2}\text{ml}/\mu\text{U}$). The estimated kernels of first (Fig. 4—dotted) and second order for the noise free case are almost identical to the true kernels given by Eqs. (17) and (18) (Fig. 2—top panel).

In order to examine the effect of measurement noise on the kernel estimates, we repeat the kernel estimation with the aforementioned input-output data after the addition of 20 independent white-noise signals with maximum amplitude equal to approximately 20 % of the basal glucose value (i.e., error range of ±16 mg/dl) to the output [21]. This corresponds to an SNR of around 6.5 dB relative to the demeaned glucose deviations output. The resulting kernel estimates are also shown in Fig. 4 (top panels) and demonstrate the robustness of this modeling approach in the presence of measurement noise. The corresponding linear and nonlinear NMSEs are equal to 24.0 ± 2.7 and 23.6 ± 2.7 % respectively (mean ± standard deviation), i.e., the output additive noise is not accounted by the model. Also in Fig. 4 (bottom panels), we present the kernel estimates obtained with an insulin input of the same length (144 points) composed of a random sequence of impulses (representing insulin concentration increases that could be due to insulin infusions), with a mean frequency of 1 impulse every 2 h and a normally distributed random amplitude with

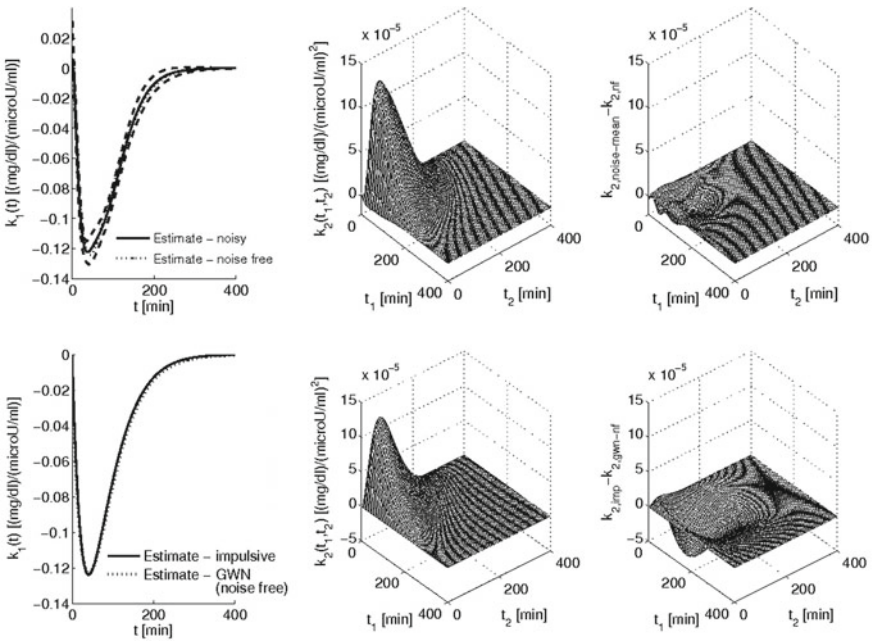

Fig. 4 *Top panel* The estimated first and second order Volterra kernels of the MM using a GWN input of 144 points (12 h) when 20 different realizations of independent GWN signals are added to the output for an SNR of 6.5 dB. The obtained first-order (*left panel—solid* mean value, *dashed* ± one standard deviation, *dotted* noise-free estimate) and second-order kernel estimates (*middle panel*—mean value, *right panel* standard deviation) are not affected significantly relative to their exact counterparts (Fig. 1—top panel), demonstrating the robustness of this approach. *Bottom panel* The estimated first and second order Volterra kernels of the MM for an insulin input composed of 8 insulin infusions over 12 h. The timing and amplitude of each infusion are random (see text). Note the similarity of these estimates to the estimates obtained from GWN inputs

standard deviation 20 μU/ml. The resulting kernel estimates are almost identical to their GWN-input counterparts, demonstrating the feasibility of estimating accurate Volterra models using sparser, infusion-like stimuli.

3.5 Simulation Results: Closed-Loop Model

The closed-loop AMM was simulated by numerical integration of Eqs. (3)–(5), using the same GWN input used for the open-loop MM. The parameter values used for this model were $p_1 = 0.020\ \text{min}^{-1}$, $p_2 = 0.028\ \text{min}^{-1}$, $p_3 = 10^{-4}\ \text{min}^{-2}\text{ml}/\mu\text{U}$ and parameter values of $a = 0.13\ \text{min}^{-1}$, $\beta = 0.05\ \mu\text{U-min}^{-2}/\text{ml}$ per mg/dl, $\theta = 80$ mg/dl for the additional insulin-secretion equation. Representative time-series data of the resulting insulin input, insulin secretion, insulin action and glucose, used for training the equivalent LVN model, are shown in Fig. 5, where the effect

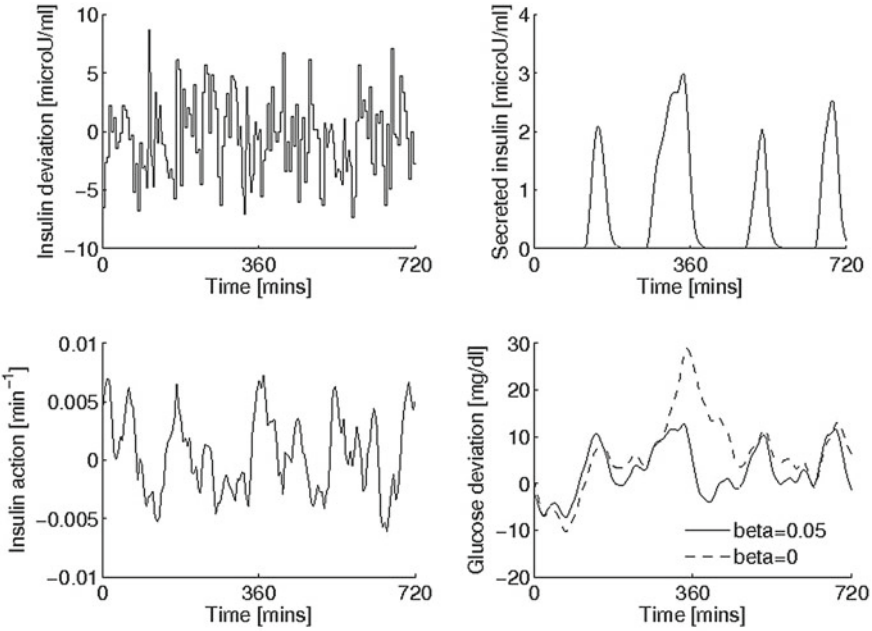

Fig. 5 Representative realization of the closed-loop AMM time-series data for a GWN insulin input used for LVN training (length: 12 h). The insulin time series represent deviations from its basal value. The effect of the secretion equation is seen by comparing the two output waveforms of glucose deviations shown in the bottom right panel (*dashed* open-loop, *solid* closed-loop for $\beta = 0.05$)

of insulin secretion, relative to the open-loop case, can be seen in the bottom right panel (solid: closed-loop output, dashed: open-loop output).

An LVN with $L = 5$, $K = 2$ and $Q = 3$ was employed in this case—i.e., a more complex structure of higher order is required relative to the open-loop case. In the noise-free case, the obtained nonlinear model reduces the prediction NMSE considerably, from 12.41 %—yielded by the linear model—to 2.18 % (Fig. 6, top left panel). As before, we repeat the kernel estimation after adding 20 independent white noise sample signals (with the same variance as above) to the output. Note that the resulting SNR is now around 4.5 dB, i.e. lower than the open-loop case, since the noise-free output (glucose deviations) has a smaller mean-square value in the closed-loop case, due to the effect of the endogenous insulin secretion. Therefore, the corresponding NMSEs are larger—i.e. 48.2 % for the linear model and 34.2 $\pm$ 4.0 % for the nonlinear model—and correspond, for the nonlinear model, to the noise present in the signal. This demonstrates the predictive capability of the obtained models in the presence of considerable output-additive noise that emulates the observed errors in the measurements of current continuous glucose monitors [21]. The kernel estimates for both cases are shown in Fig. 6, illustrating the robustness of this approach. The first and second order kernels of the closed-loop AMM exhibit biphasic characteristics (i.e., regions of positive and

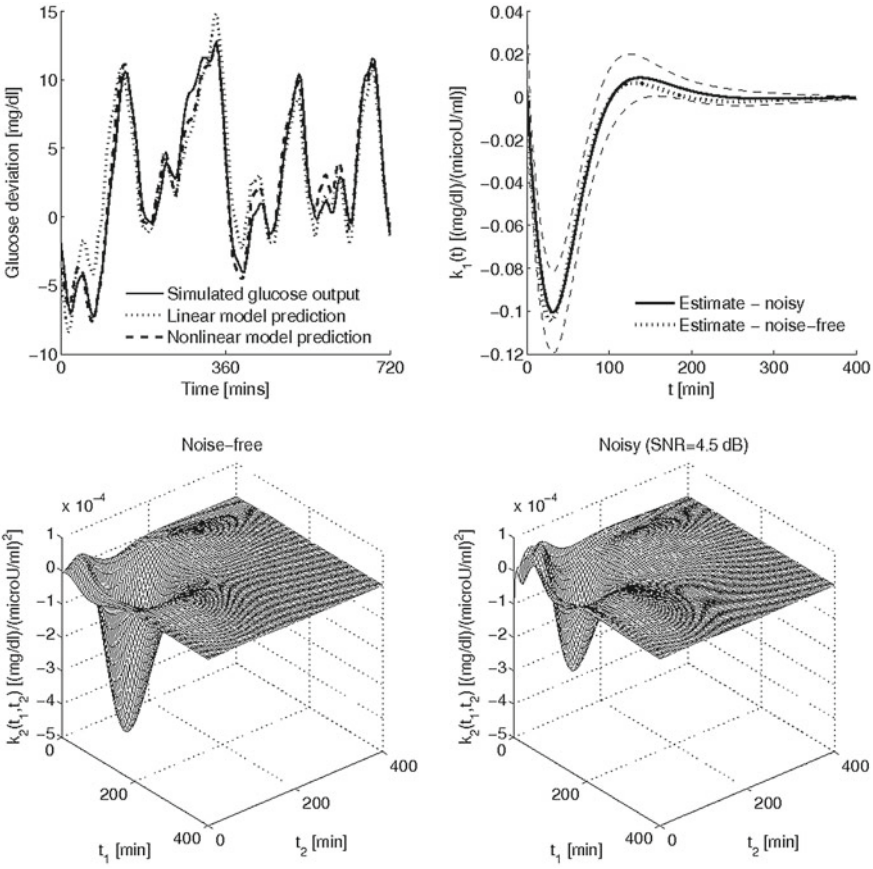

Fig. 6 Representative model predictions (noise-free output, *top left*) and estimated first and second order Volterra kernels of the closed-loop AMM for a GWN input of 144 points (12 h) for noise-free output (*top right—dotted* and *bottom left*) and when 20 different realizations of independent GWN measurement noise are added to the output for an SNR of 4.5 dB (*top right—solid black* mean, *dashed black* ± one standard deviation and *bottom right*—mean). Nonlinear models achieve better predictions (over 10 % NMSE reduction). The obtained kernel estimates are not affected significantly relative to their noise-free counterparts despite the low SNR

negative response to a positive change in the input, and vice versa). The first-order kernel contribution to the output remains dominant over the second-order kernel contribution for impulsive inputs up to about 100 μU/ml.

3.6 Simulation Results: Principal Dynamic Mode Models

The obtained equivalent PDM models for both the open-loop and closed-loop models are shown in Fig. 7. In the open-loop case (top panel), since we have used $K = 1$ in the LVN model, the equivalent PDM model has one branch, with the

PDM dynamics exhibiting similar characteristics to the open-loop first-order kernel (Fig. 7) and the static nonlinearity being close to linear, due to the relatively low value of p_3 used in this particular case. In the closed-loop case (bottom panel), we have used $K = 2$; therefore, the equivalent PDM model has two branches. The lower PDM exhibits a clear biphasic response characteristic (corresponding to a glucose decrease and increase respectively, in response to an insulin increase) that is not present in the open-loop model. The upper PDM branch exhibits slower dynamics (peak latency of about 80 min) than the open-loop PDM (peak latency at 40 min) and a strictly negative nonlinearity (i.e., always leading to a reduction of glucose), while the nonlinearity of the open-loop model has both positive and negative response regions. The PDM of the lower branch exhibits faster dynamics (shorter latency of the first peak of about 30 min) and has a nonlinearity that resembles a sigmoidal (soft saturating) characteristic.

3.7 Simulation Results: Sorensen Model

Finally, we present results from fitting the MM and LVN models to simulated data obtained from the model proposed by Sorensen [38], which has been used as a comprehensive representation of the metabolic system in several studies (e.g., [25, 35]) for insulin input signals considered above (i.e., random insulin variations around a putative basal value). Note that we do not make claims about the universal validity of this particular model, but we use it as a third-party metabolic simulator for comparative purposes. We considered two distinct cases of Sorensen model parameters: one that corresponds to a healthy subject and another that corresponds to a Type-1 diabetic subject, following the procedure described in [26]. Briefly, Type 1 diabetes is characterized by complete failure of the pancreatic beta cells, decreased (40–50 % of normal) insulin stimulated hepatic and periphery glucose uptake and impaired, glucose-induced, endogenous glucagon production (assumed 50 % of normal in this study). Therefore, the corresponding parameters in Sorensen's model were changed accordingly [26].

The MM parameters were obtained by using a nonlinear optimization method (Levenberg-Marquardt method) in order to fit p_1, p_2 and p_3 to the Sorensen model generated data. We considered 10 different realizations of the insulin input signal (of the same length considered above) and provide the results in Fig. 8. The results show that the output prediction performance of the LVN model is superior in both cases, particularly for the Type-1 diabetic case. Specifically, the average NMSEs for the LVN approach were equal to 3.62 ± 1.92 % and 4.95 ± 4.90 % for the healthy and Type-I diabetic cases respectively, while for the MM approach the corresponding NMSEs were equal to 11.11 ± 7.52 % and 25.37 ± 10.73 %, i.e., considerably higher. We note that an LVN model structure with $L = 5$, $K = 1$ and $Q = 2$ was deemed appropriate in this case.

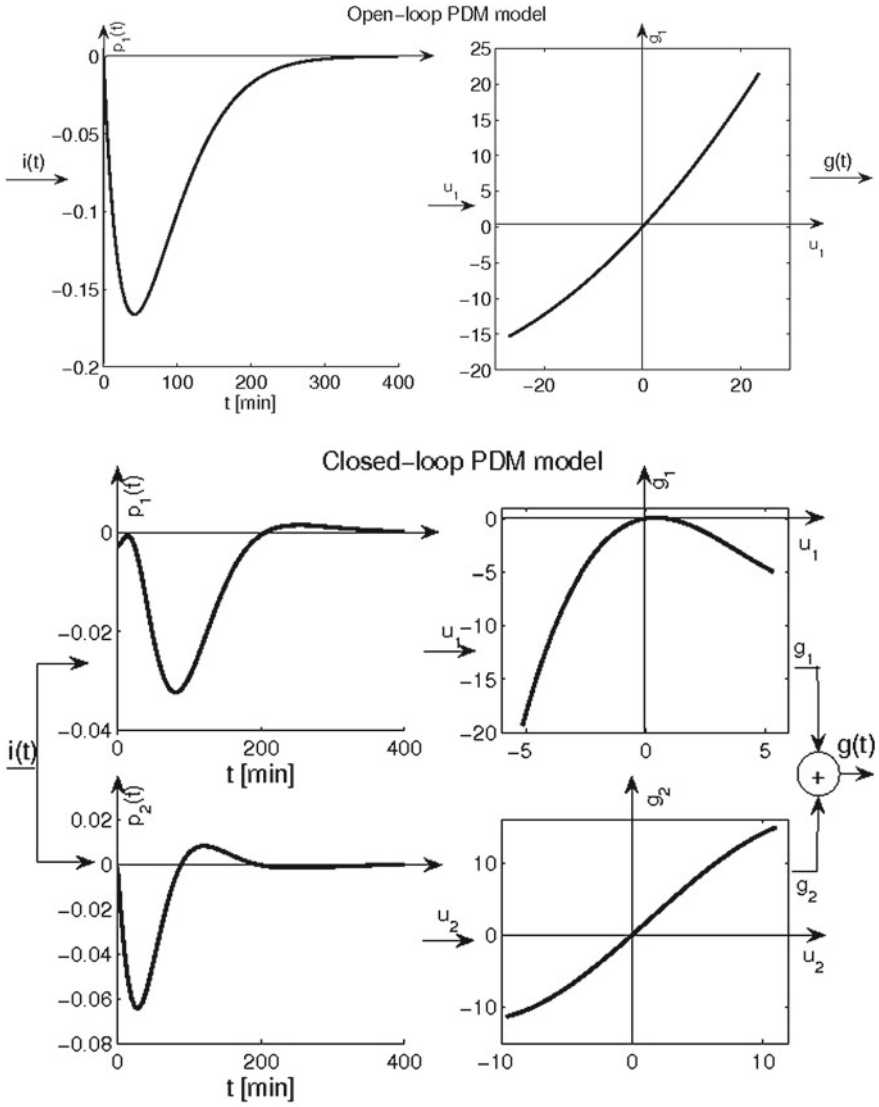

Fig. 7 The obtained PDM model for the open- and closed-loop models, which consist of one and two branches (*top* and *bottom panels* respectively). The open-loop single PDM (*top left panel*) exhibits a glucoleptic characteristic (reduces the glucose output) for positive insulin inputs in a mildly sublinear manner. The closed-loop upper PDM branch exhibits a glucoleptic characteristic for positive or negative insulin inputs in a mildly supralinear manner, unlike the single PDM branch of the open-loop MM. Note that the latency of the peak response (about 80 min) is much longer for this closed-loop PDM than for the open-loop PDM (about 40 min), and the slope of its output nonlinearity is different for positive/negative input (about 4 to 1). The lower PDM is biphasic with the first glucoleptic peak having a latency comparable to the open-loop PDM (about 30 min) and the second glucogenic peak being much smaller (about 15 %) and having a latency of about 120 min. The nonlinearity of the lower PDM branch retains the biphasic response characteristic (increase of insulin leads to glucose decrease and vice versa) and is mildly sublinear (resembling a soft saturating characteristic)

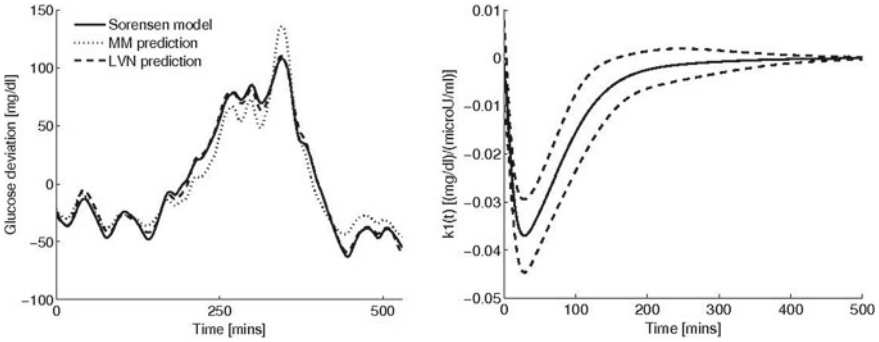

Fig. 8 The predictions of the MM and LVN models for a representative Sorensen-model simulated data set (healthy subject; *left panel*) and the average first-order kernel estimate of the LVN model for 10 different insulin input realizations (*right panel—solid black* mean *dashed line* ± one standard deviation)

4 Insulin-Glucose Dynamics in a Fasting Dog

4.1 Experimental Data Collection and Analysis

Plasma glucose and insulin were measured in a healthy male mongrel dog every 3 min over a 10-h period (200 samples). The data were collected under conditions of spontaneous activity (there were no insulin or glucose injections). The animal was judged to be in good health by visual observation, weight stability, body temperature, and hematocrit. The University of Southern California Institutional Animal Care Committee approved all surgical and experimental procedures. The dog was fed standard can food and had free access to standard dry chow and tap water. A chronic catheter (Tygon, ID = 0.13 cm) was implanted one week prior to the experiment. The catheter was placed into the femoral vein and advanced into the inferior vena cava and tunneled subcutaneously to the neck and exteriorized. The experiments were performed in the morning after a 12 h fast and the dog was not fed during the experiment. One hour prior to the beginning of blood sampling, an infusion of 500 ml 0.9 % saline was given to avoid dehydration of the animal due to the extended fast. Arterial blood was sampled at 3-minute intervals for 10 h from 6:00 a.m. till 4:00 p.m. Heart rate and blood pressure were monitored every 30 min over the entire experimental period. Samples were collected in tubes containing EDTA and 0.275 mg/ml lipoprotein lipase inhibitor paraoxon to avoid in vitro lipolysis. Samples were immediately centrifuged, and the plasma separated and stored at −20 °C. Plasma glucose was analyzed by the glucose oxidase method on an automated analyzer (model 23A, Yellow Springs Instruments). Insulin was measured in singlicate by an enzyme-linked immunospecific assay (ELISA, CV = 2 %) originally developed for human plasma by Novo-Nordisk and adapted for dog plasma. The collected insulin/glucose time-series data are

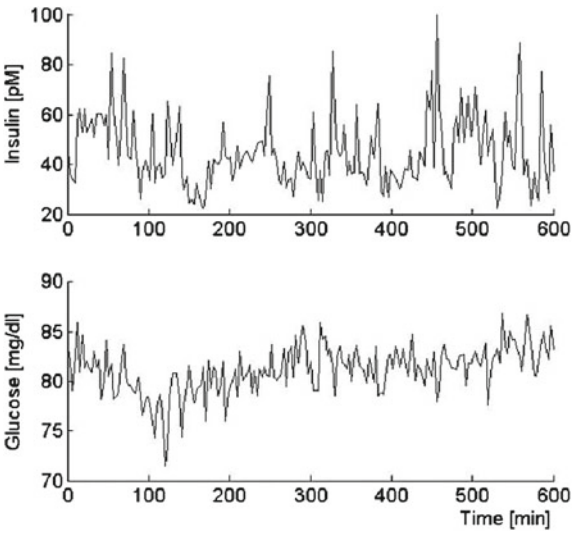

Fig. 9 Experimental time-series data of plasma insulin (*top panel*) and glucose (*bottom panel*) collected from a fasting dog over 10 h (sampling interval is 3 min)

shown in Fig. 9. All signals were demeaned prior to processing and the means were considered to be the respective basal values.

The time-series data were analyzed using the LVN methodology outlined above (Sect. 2.3) in both causal directions (i.e. when the spontaneous plasma insulin variations are viewed as the input and the plasma glucose variations are viewed as the output, and when the roles of input and output are reversed). The LVN model contains the Laguerre parameter α (between 0 and 1), which determines the rate of relaxation of the Laguerre functions. We utilized an LVN model with two filter-banks with distinct α parameter values [31], in order to capture the identified fast and slow dynamics between insulin and glucose [36] efficiently. The resulting Volterra-equivalent model has predictive capability for all possible inputs within the dynamic range of the data used for its estimation. The structural parameters of the LVN model were selected through the search procedure described above (Sect. 2.3). After training the LVN model with the insulin-glucose data, equivalent PDM models (Eq. 12) were obtained in both causal directions.

4.2 Insulin-to-Glucose Branch

The mean and standard deviation of the plasma insulin and glucose data were equal to 44.9 ± 13.8 pM and 81.1 ± 2.4 mg/d1 (mean ± standard deviation) respectively. Figure 10 shows the estimated modular PDM model for the insulin-to-glucose relationship. The structural parameters L, K and Q of the model were selected as follows: two Laguerre functions for each filter bank ($L_1 = L_2 = 2$), two parallel PDM branches ($K = 2$) and cubic nonlinearity ($Q = 3$). The abscissa of the

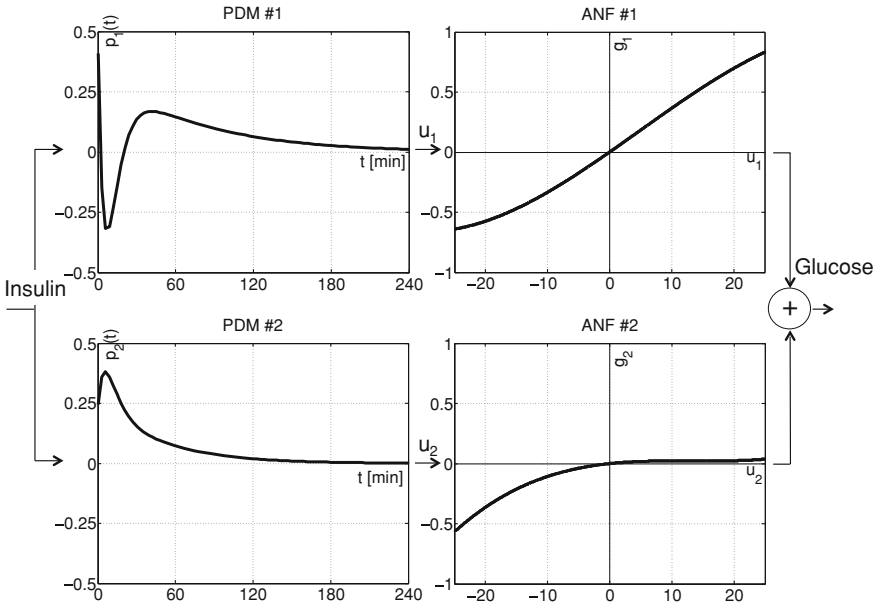

Fig. 10 The insulin-to-glucose model is composed of two branches, each of which is the cascade of a linear filter (PDM) followed by a static nonlinearity (ANF). The upper branch consists of an early glucoleptic response to insulin increases, followed by a subsequent glucogenic response, while the lower branch produces non-zero responses to negative insulin deflections only, due to the halfwave rectifying characteristic of the corresponding nonlinearity. The input signal (plasma insulin) and the output signal (plasma glucose) represent deviations from the respective basal values that are computed as the mean values of the recorded data and subtracted prior to processing

k-th static nonlinearity f_k is the output u_k of the k-th PDM filter p_k and the ordinate is the respective additive component $g_k(t)$ of the model output. The input and output signals (plasma insulin and glucose respectively) of this model represent deviations from the respective mean values that were subtracted prior to model estimation.

The obtained PDM model suggests the correspondence of the upper branch to the primary effect of insulin on plasma glucose. Specifically, the PDM of this branch exhibits an early glucoleptic phase, i.e. it causes reduction of glucose levels in response to an increase of insulin that is due to insulin-facilitated uptake of glucose by tissue cells and glycogen synthesis in the liver, over the first 20–25 min (with a trough at 10 min). It also exhibits a subsequent glucogenic phase that extends over about 150 min, which describes mainly the processes of production and release in the blood of new glucose by the liver and other organs (glucogenesis) in response to insulin increases. In general, the biphasic form of this PDM suggests there is counter-regulation of glucose changes in response to insulin deflections due to the closed-loop nature of insulin-glucose interactions. The

respective static nonlinearity (ANF#1) is odd-symmetric and it consists of a linear part, as well as a soft saturating characteristic. The form of the second branch suggests that it produces a glucose reduction in response to negative deflections of insulin only, as its respective nonlinearity exhibits a negative half-wave rectifying characteristic. The latter assures the reduction of plasma glucose in response to a negative deflection of plasma insulin from the basal value, since this generates a negative value in the output u_2 of PDM#2, but no major change in glucose for a positive deflection of plasma insulin from the basal value. Combined with the characteristics of the upper branch, the characteristics of the lower branch suggest that the response of the two model branches to insulin concentration reductions are antagonistic and may serve to regulate the overall glucose response.

In order to illustrate the net effect of both branches to a simple insulin input, we show the total model-predicted glucose response to an impulse of insulin with amplitude of 10 pM, which corresponds to around 1 standard deviation of the actual experimental insulin data, in Fig. 11. The overall response exhibits an early reduction of blood glucose followed by an overshoot and settles to zero after around 200 mins and it resembles in waveform the upper-branch PDM as expected, since a positive insulin input will elicit no contribution from PDM#2 (Fig. 11).

The normalized mean-square error (NMSE) of the output prediction of this third-order PDM model was 60.2 %, while the linear model prediction NMSE was 89.9 %—a fact that indicates the presence of strong nonlinearities in the causal relation of insulin-to-glucose variations. The glucose variations not explained by the model (i.e., not caused by prior insulin variations) are the residuals of the model prediction, which are viewed as "glucose disturbances" caused by numerous internal and external factors (hormonal, neural, metabolic) that are not insulin-dependent. Moreover, the effect of measurement errors may be considerable; for instance, the reader is referred to [12] for a quantitative description of the performance of the glucose analyzer used in the present experiment. The relatively high NMSE value of the overall output prediction indicates that the contributions of these insulin-independent unobserved factors, as well as the effects of measurement errors are significant.

4.3 Glucose-to-Insulin Branch

We next examine the reverse causal pathway, i.e. how variations of plasma glucose (input) affect the variations of plasma insulin (output), using the same experimental data. The obtained PDM model of the glucose-to-insulin causal relationship is shown in Fig. 12 and has two PDM branches. The PDM of the upper branch is almost monophasic (with the exception of the zero-lag value that seems to counterbalance the zero-lag value of the lower-branch PDM) and causes a co-directional change of insulin for a change of glucose, consistent with our understanding of the function of pancreatic beta cells. The PDM-ANF cascade of

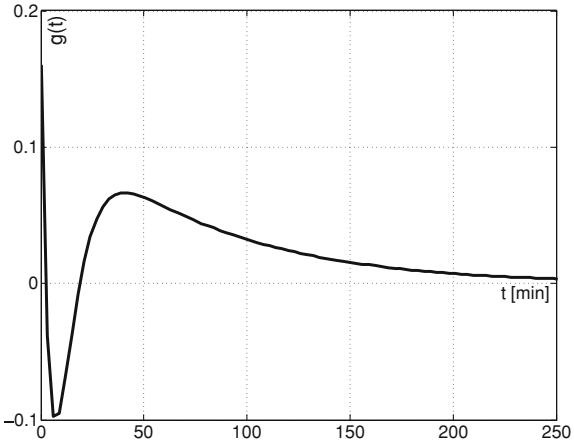

Fig. 11 Prediction of the insulin-to-glucose model (Fig. 10) to an impulse insulin input with amplitude 10 pM (around 1 standard deviation of the experimental data). The output waveform $g(t)$ resembles the form of the upper branch PDM of the model

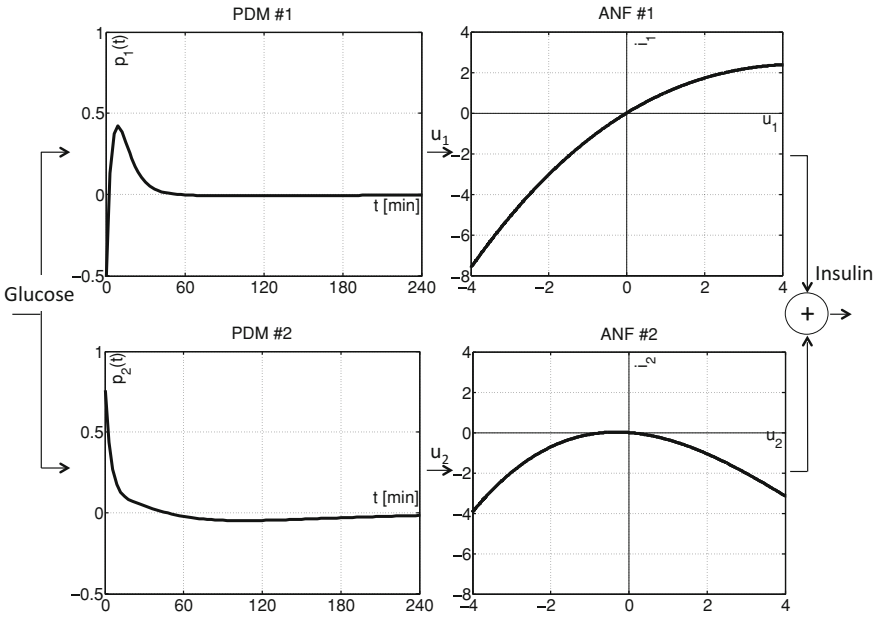

Fig. 12 The glucose-to-insulin model is composed of two PDM branches, the first of which causes a co-directional change of insulin for a change of glucose, while the second is strictly insulinoleptic, i.e. it causes reduction of insulin to either positive or negative change of glucose

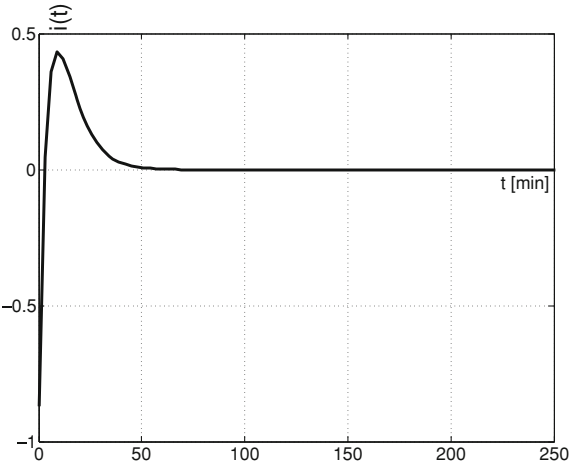

Fig. 13 Prediction of the glucose-to-insulin model (Fig. 12) to a glucose impulse insulin input with amplitude 1 mg/dl (around 0.5 standard deviations of the experimental data)

the lower branch is strictly insulinoleptic (i.e. it causes reduction of insulin to either positive or negative change of glucose) and operates in two time-scales: one fast over 10–15 min and the other slow over around 2 h.

Figure 13 shows the model-predicted insulin response to a positive impulse of glucose with amplitude of 1 mg/dl (around half the standard deviation of the actual experimental data). The model prediction resembles in waveform the upper-branch PDM of Fig. 12, since an increase of glucose is expected to elicit an increase of insulin by stimulating pancreatic secretion. In general, the second branch of both the above models (Figs. 11 and 13) appears to have a counter-regulatory role, balancing the effect of the respective first branch of each model. The model prediction achieved by the PDM model of Fig. 12 is equal to 69.9 %, while the corresponding linear NMSE is equal to 97.6 %. This implies a predominantly nonlinear relationship between glucose and insulin. The large nonlinear NMSE value suggests that spontaneous plasma glucose variations account for a fraction of spontaneous insulin variations, and that interferences from other physiological variables dominate in the formation of the insulin signal, along with the aforementioned possible effects of measurement errors.

5 Discussion

In the present chapter, we have rigorously examined the relation between nonlinear compartmental and Volterra models of glucose metabolism. We have also applied the proposed data-driven approach to investigating the spontaneous dynamic interactions between insulin and glucose in a fasting dog. Two widely used compartmental models, the minimal model (MM) of glucose disappearance and its closed-loop extension (AMM), which includes the effects of insulin

secretion, were formulated in the Volterra-Wiener framework and equivalent descriptions, in the form of Volterra models, were derived analytically. The effect of parametric model parameters of clinical importance on these descriptors (Volterra kernels) was examined. Using simulated data generated from the aforementioned compartmental models using both random-like and impulsive insulin stimuli, as well as the experimental dog data, we have demonstrated the feasibility of obtaining Volterra models that describe these data accurately. We have also shown that these estimates are not affected significantly by output-additive noise corresponding to measurement noise. The results provide evidence that Volterra models, free of a priori assumptions, may be estimated reliably from patient-specific data. These models may provide quantitative descriptions that reflect the underlying physiological mechanisms under general operating conditions and may prove useful in diagnostic or therapeutic [27] applications. We should note that for model-based glucose control applications, additional factors, such as the delay between plasma glucose and the sensor signal, should be taken into account.

5.1 Comparison Between Compartmental and Volterra Models

The parametric models examined herein are nonlinear due to the presence of a bilinear term in Eqs. (1) and (3), which modulates the effective time constant of glucose disappearance and depends on the action of plasma insulin (in the case of MM) and both plasma and endogenous secreted insulin (in the case of AMM) respectively. An additional nonlinearity is found in the endogenous insulin secretion Eq. (5) of the AMM in the form of a nonlinear threshold operator. The range of values for the MM and AMM parameters is taken from the literature [3, 4, 20, 25, 41, 45]. The value of p_3 was selected towards the upper limit of previously reported values in order to increase the contribution of the bilinear term, while the parameter β in Eq. (5), which determines feedback strength was selected to be larger than the value reported in [45] since, for the stimuli examined in the present paper, the effect of endogenous insulin was almost negligible for this latter value (it corresponds to low tolerance, obese patients [45]). Note that in the more general case, the value of β could be viewed as being dependent on g, in order to account for the effect of blood glucose concentration on insulin secretion. The value of the threshold β in the endogenous insulin secretion Eq. (5) was selected equal to zero in order to simplify the analytical derivations. This threshold can be generally set to a larger value, particularly when glucose disturbance terms that are non-insulin dependent, are included. However, in the context of the simulations presented herein, this value yielded reasonable patterns for the insulin secretion profile (Fig. 5).

Two types of inputs (variations of insulin concentration) were used in this computational study for the simulation of the parametric models: GWN fluctuations around a putative basal value (corresponding to the GWN mean) and random sequences of sparse insulin increases (about one every 2 h on the average), which may result from insulin/glucose infusions. It was shown that reliable and robust nonparametric models can be obtained with both types of stimuli in the presence of measurement noise. The GWN insulin fluctuations may also be viewed as internal spontaneous fluctuations and, therefore, the applicability of this approach can be extended to the case of spontaneous glucose/insulin measurements. The use of random sequences of larger sparse impulsive insulin increases, although unconventional, was shown to be effective in terms of model estimation and may offer clinical advantages as it is likely to mitigate the risk of induced hypoglycemia—an issue that must be examined carefully in future studies.

The Volterra approach does not require specific prior postulates of compartmental model structures (e.g. it is not committed to any particular number of compartments) and allows estimation of the model (i.e. the Volterra kernels) directly from arbitrary input-output data. Therefore, it offers the advantage of yielding models that are "true-to-the-data" and valid under all input conditions within the range of the experimental data. Therefore, this fundamentally different approach provides significant benefits relative to existing approaches in terms of modeling flexibility and accuracy.

The robustness of the Volterra modeling approach (i.e. the effect of output-additive noise on the obtained kernel estimates) was studied by selecting as noise sample signals from a GWN process with variance consistent with what is known about glucose measurement errors (i.e. a standard deviation equal to 14–20 % of the glucose basal value [21]). However, we must make the distinction between noise (which is primarily related to measurement errors) and systemic disturbance (which is related to systemic perturbations that are not explicitly accounted for in the model). The systemic disturbance signal may include the effect of meals [17], the effect of circadian and ultradian endocrine cycles [44] and the effect of randomly occurring events of accelerated metabolism (due to exercise or physical exertion) as well as neuro-hormonal excretions (due to stress or mental exertion). The amplitudes and the relative phases of these disturbance components will generally vary among subjects and over time. Since the selection of such disturbance components is rather complex, the study of their effect on the robustness of the model estimation is deferred to future studies.

The MM approach is based on the notion that estimates of the three model parameters (p_1, p_2 and p_3), obtained through a glucose tolerance test, provide the necessary clinical information for diagnostic purposes in the form of the equivalent indices of glucose effectiveness (S_G) and insulin sensitivity (S_I). Although this proposition has merit and has proven to be useful so far, it is widely recognized that it has serious limitations [10, 11]. To overcome some of these potential limitations, our approach advances the notion that a Volterra-type model (in the form of kernels or the PDM model) provides the requisite clinical information in a more complete manner (i.e., no model constraints). In order to compare the

relative utility of the Volterra approach with the conventional MM approach in a clinical context, we must define clinically relevant attributes for the two approaches that are directly comparable. For instance, if we are interested in deriving quantitative descriptions/measures of how insulin affects the plasma glucose concentration in specific subjects (i.e. based on collected data), we may use certain features of the estimated first-order kernels, such as the integrated area, peak value and initial slope, which determine the linear component of the overall effect of an insulin injection, its maximum instantaneous effect and how fast this effect occurs respectively, instead of the estimated MM parameters.

In this context, the combined effect of errors in the estimates of the three parameters of the MM (p_1, p_2, p_3) may be compared to estimation errors in the integrated area of the first-order kernel, which is equal to the ratio S_I/S_G (i.e. $p_3/(p_1p_2)$), as a measure of how much a unitary insulin impulse will affect the plasma glucose concentration. Also, since $S_G = p_1$ is the inverse of the long time-constant of the kernel (providing a measure of the extent of the kernel), it follows that "insulin sensitivity" S_I is akin to the average kernel value. Thus, one may suggest that the clinical index of "insulin sensitivity" may be defined alternatively by the average kernel value and "glucose effectiveness" by the extent of the kernel in the data-driven modeling context. It also stands to reason that the peak value of this kernel is likely to have some clinical significance, since it quantifies the maximum effect of an insulin injection on blood glucose in a given subject. Finally, the slope of the first-order kernel at the origin (a measure of how rapidly glucose drops in response to an insulin infusion) is equal to $-(g_b p_3)$. Since the basal glucose value is known, a quick estimate of p_3 can be obtained from the slope of the first-order kernel. In the above context, PDM models (Figs. 7, 8, 9, 10, 12) may prove very beneficial, since they facilitate meaningful physiological interpretations relative to the general Volterra formulation. Therefore, certain characteristics of the PDM branches (e.g., the dynamics of the linear filters and the characteristics of the nonlinearities) may also be associated to clinical indices that describe insulin action and its efficiency in specific subjects.

Existing insulin-glucose models can be divided in two broad categories; the first includes models that describe these dynamics in a simplified manner by using a limited number of parameters of diagnostic importance, in order to make these parameters identifiable from relatively simple experimental protocols (IVGTT, OGTT, EHC) and the second category includes more complicated models that capture the complexity of the underlying physiology under more general operating conditions. Choosing the most appropriate model type depends strongly on the particular application. For instance, minimal-type models have met with success for diagnostic purposes; however, they do not describe the metabolic system realistically. On the other hand, more complicated models achieve this but they are typically not identifiable from experimental data that are available in practice, requiring considerably more complicated protocols (such as multiple tracer experiments).

It is worth noting that a recent large-scale model by Dalla Man et al. [14] has been approved by the Food and Drug Administration Agency of the USA and the

Juvenile Diabetes Research Foundation as a substitute for clinical trials for the preclinical testing of glucose control algorithms, illustrating the importance of mathematical modeling. In our view, data-driven models, such as the ones presented hereby, present an attractive alternative that lies between the two aforementioned main model categories. Data-driven models are identifiable in practical settings in a patient-specific and adaptive manner, and provide more flexibility than minimal-type models. However, they are not based on physiological considerations; therefore this flexibility should be exploited carefully and their complexity should be selected judiciously in order to assure that they are accurately describing the underlying phenomena without overfitting to particular data sets.

5.2 Insulin-Glucose Dynamics in a Fasting Dog

There are four salient issues that deserve further elaboration and discussion: (1) the validity and utility of the obtained models; (2) the notion of "indirect effects" captured by the model of a closed-loop system; (3) the physiological interpretation of the obtained PDMs and (4) the pivotal role of internal "disturbance" signals in closed-loop systems. These issues are intertwined and their successful resolution will determine the potential utility of the advocated approach.

The validity of the obtained model is based on its predictive capability and the consistency of the modeling results across different experiments. Random-like spontaneous variations enable us to perform broadband analysis of the input-output data and obtain reliable models that are capable of predicting the output for arbitrary inputs within the dynamic range of the available measurements, removing the restrictive effect of specialized test inputs (such as impulses or sinusoids). The significant reduction in the prediction NMSE achieved by nonlinear models (especially for the glucose-to-insulin branch) suggests the presence of strong dynamic nonlinearities. This reduction is unlikely to be due to overfitting, which is an issue that may arise when using nonlinear models to model short experimental data records. The number of free parameters for the LVN approach depends linearly on system order [31], and is much lower compared to alternative approaches, such as standard function expansions or orthogonal based approaches, for which the same dependence is exponential [30]. The free parameters of the linear and nonlinear models examined herein were equal to 25 and 29 respectively, i.e. third-order models required the estimation of 4 additional parameters only. The availability of data from one dog, as well as the relatively limited dynamic range of the experimental data limits our ability to generalize our findings; however, the unique nature of the employed data yields novel insights regarding the dynamic interactions between spontaneous insulin and glucose fluctuations.

The notion of indirect effects is fundamental in the context of closed-loop physiological systems, which are observed under conditions of spontaneous activity. Multiple physiological processes participate in the transition of the system to the state of dynamic equilibrium (homeostasis). These processes are typically

nonlinear, dynamic and interacting in a complex manner. Therefore, a change in one of the implicated variables will generally cause some direct effects (immediate consequences) and indirect effects (subsequent consequences of a chain of events). The indirect effects are harder to notice/delineate experimentally and even harder to analyze, since the number of overlapping effects from interacting factors increases with system complexity. The advocated approach offers the practical means for obtaining a unique glance of these indirect effects in a quantitative and reliable manner, as illustrated in the cases of the glucogenic and insulinogenic branches of the insulin- to-glucose and glucose-to-insulin models.

The physiological interpretation of the obtained PDM models attains critical importance for the advancement of scientific understanding as well as their potential use for improved clinical diagnosis. The ability to detect subtle early defects in the complex cascade of metabolic events involved in insulin and glucose regulation may prove crucial for the improved diagnosis of diseases such as Type II diabetes [36]. The presented models quantify the relation between naturally occurring insulin/glucose variations and may be used to identify changes in the glucose effectiveness and insulin sensitivity of a subject—thus leading to improved diagnostic methods. They may also disclose physiological deficiencies (e.g. an undeveloped glucoleptic or insulinogenic component) in a quantitative manner. The potential clinical utility can be expanded if additional physiological variables are incorporated (e.g. free fatty acids). The dynamic characteristics of the PDM model, which exhibit multiple time constants (Figs. 10 and 12), are in agreement with the previously reported entrainment between insulin and glucose patterns over different time scales (rapid to ultradian) [36, 40]. In these studies, experimental impulsive or step stimuli were induced, whereas in the present study we studied natural variations, an approach that removes the need for such interventions.

The role of internal "disturbance" signals is pivotal for closed-loop physiological systems seeking homeostasis. Although homeostasis is typically mediated through multiple nested closed-loops, let us consider the case of two physiological variables operating in a closed-loop configuration (e.g. insulin and glucose) as shown schematically in Fig. 14. The two measured variables (spontaneous variations of plasma insulin $I(t)$ and plasma glucose $G(t)$, are causally linked in a mutual interdependence described by the general system operators **A** and **B**. Operator **A** transforms the insulin signal $I(t)$ into the causally linked (i.e. insulin-dependent) glucose component $G_c(t)$ in a dynamic and nonlinear fashion. Likewise, operator **B** transforms the glucose signal $G(t)$ into the causally linked (i.e. glucose-dependent) insulin component $I_c(t)$. Each of these nonlinear dynamic operators can be described by a Volterra-equivalent model (such as the PDM models of Figs. 10 and 12) that is estimated directly from spontaneous input-output data. The model residuals of the two operators (Figs. 11 and 13) are the "disturbance" signals, $G_d(t)$ for glucose and $I_d(t)$ for insulin, that represent the aggregate effects of multiple systemic factors (e.g. glucagon, cortisol, epinephrine etc.) and external factors (e.g. meals, exercise, stress, mental exertion etc.). These disturbance signals are added to the causally linked

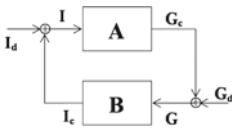

Fig. 14 The closed-loop configuration representing the plasma insulin-glucose dynamic interactions (glucose-to-insulin and insulin-to-glucose models, **B** and **A** respectively). The "disturbance" signals I_d and G_d are the residuals of the obtained causal models and represent the aggregate effects of multiple internal (e.g. glucagon, epinephrine, norepinephrine, cortisol, growth hormone, somatostatin etc.) and external factors (e.g. meals, exercise, stress, mental exertion etc.)

components, $G_c(t)$ and $I_c(t)$ (Figs. 11 and 13, left panels), to form the observed variables $G(t)$ and $I(t)$, respectively.

Regarding the overall functional characteristics of the closed-loop configuration of Fig. 14, we examine the closed-loop relation in operator notation:

$$G(t) = \mathbf{A}[\mathbf{B}[\mathrm{G(t)}] + \mathrm{I_d(t)}] + \mathrm{G_d(t)} \tag{26}$$

where $\mathbf{B}[G(t)]$ denotes that the operator **B** (glucose-to-insulin PDM model) acts on the glucose signal $G(t)$. Equation (26) is equivalent to a nonlinear auto-regressive model with exogenous input (NARX) with stochastic terms due to the interaction of $I_d(t)$ with **A**.

6 Conclusion

Mathematical modeling has played a central role in the context of diabetes diagnosis and treatment. The results of the present chapter demonstrate the relative advantages and disadvantages of the Volterra modeling methodology versus the compartmental approach for specific minimal-type parametric models (MM and AMM). The Volterra approach is inductive (data-driven) and yields models with minimum prior assumptions. The compartmental approach is deductive (hypothesis-based) and yields models with the desired level of complexity that are directly interpretable but not necessarily inclusive of all functional characteristics of the system. The recent availability of continuous measurements of glucose (through continuous glucose sensors) and the feasibility of frequent infusions of insulin (through implantable insulin micro-pumps) make possible the realistic application of data-driven modeling approaches in a subject-specific and adaptive context, which does not require the prior postulates of compartmental models. The potential benefits include: (i) the inherent completeness of the obtained models, in the sense that they will include all functional characteristics of the system contained within the data (ii) the robustness of their estimation in a practical context (iii) their subject-specific customization and (iv) their time-dependent adaptability when the system characteristics are changing slowly over time, allowing for

effective tracking of these changes in each subject. This could be achieved by piecewise stationary models or by employing recursive estimation schemes, which may be readily implemented for the LVN models employed hereby.

This is corroborated by the presented models of the inter-relationships between spontaneous plasma insulin and glucose variations in a fasting dog, which offer quantitative means for advancing our scientific understanding and potentially improving clinical diagnosis and treatment of diabetes. This will depend on further validating our findings and on assigning correct physiological meaning to the various components of the obtained models. It is worth noting that data-driven methods typically require richer stimulus patterns than simple compartmental models. For instance, spontaneous physiological variability, such as the dog insulin and glucose measurements examined above, exhibits broadband characteristics that provide rich information for system operation over a wide dynamic range. However, measuring plasma insulin with a high temporal resolution in humans can not be performed easily and/or with a low cost with current technology, so developing such technologies deserves attention in future related research. Concluding, in our view the aforementioned results illustrate that the relation between data-driven and compartmental models deserves further attention in the future in order to more effectively combine and exploit the advantages of each approach in various clinical applications including diabetes diagnosis and glucose regulation.

Acknowledgements This work has been funded by the University of Cyprus internal research grant "Nonlinear, data-driven modeling and model-based control of blood glucose". The authors would like to thank Prof. Richard N. Bergman and Dr. Katrin Huecking for providing the experimental data. This work was supported in part by the NIH/NIBIB Center Grant No. P41-EB001978 to the Biomedical Simulations Resource at the University of Southern California.

References

1. Ackerman E, Gatewood LC, Rosevear JW, Molnar GD (1965) Model studies of blood-glucose regulation. Bull Math Biophys 27(Suppl):21–37
2. Andreassen S, Benn JJ, Hovorka R, Olesen KG, Carson ER (1994) A probabilistic approach to glucose prediction and insulin dose adjustment: description of metabolic model and pilot evaluation study. Comput Methods Programs Biomed 41:153–165
3. Bergman RN, Ider YZ, Bowden CR, Cobelli C (1979) Quantitative estimation of insulin sensitivity. Am J Physiol 236:E667–E677
4. Bergman RN, Phillips SM, Cobelli C (1981) Physiologic evaluation of factors controlling glucose tolerance in man: measurement of insulin sensitivity and beta-cell glucose sensitivity from the response to intravenous glucose. J Clin Invest 68:1456–1467
5. Bergman RN, Lovejoy JC (1997) The minimal model approach and determinants of glucose tolerance, vol 7. Louisiana State University Press, Baton Rouge
6. Bode BW, Sabbah HT, Gross TM, Fredrickson LP, Davidson PC (2002) Diabetes management in the new millennium using insulin pump therapy. Diab Metab Res Rev 18(Suppl. 1):S14–S20

7. Bolie VW (1961) Coefficients of normal blood glucose regulation. J Appl Physiol 16:783–788
8. Callegari T, Caumo A, Cobelli C (2003) Bayesian two-compartment and classic single-compartment minimal models: comparison on insulin modified IVGTT and effect of experiment reduction. IEEE Trans Biomed Eng 50:1301–1309
9. Carson ER, Cobelli C, Finkelstein L (1983) The mathematical modeling of endocrine-metabolic systems. Model formulation, identification and validation. Wiley, New York
10. Caumo A, Vicini P, Cobelli C (1996) Is the minimal model too minimal? Diabetologia 39:997–1000
11. Caumo A, Vicini P, Zachwieja JJ, Avogaro A, Yarasheski K, Bier DM, Cobelli C (1999) Undermodeling affects minimal model indexes: insights from a two-compartment model. Am J Physiol 276:E1171–E1193
12. Chua KS, Tan IK (1978) Plasma glucose measurement with the Yellow Springs Glucose Analyzer. Clin Chem 24(1):150–152
13. Cobelli C, Mari A (1983) Validation of mathematical models of complex endocrine-metabolic systems. A case study on a model of glucose regulation. Med Biol Eng Comput 21:390–399
14. Man CD, Rizza RA, Cobelli C (2007) Meal simulation model of the glucose-insulin system. IEEE Trans Biomed Eng 54(10):1740–1749
15. The Diabetes Control and Complications Trial Research (1993) The effect of intensive treatment of diabetes on the development and progression of long-term complications in insulin-dependent diabetes mellitus. New England J Med 329:977–986
16. Finegood DT, Tzur D (1996) Reduced glucose effectiveness associated with reduced insulin release: an artifact of the minimal-model method. Am J Physiol Endocrinol Metab 271(3):E485–E495
17. Fisher ME (1991) A semiclosed-loop algorithm for the control of blood glucose levels in diabetics. IEEE Trans Biomed Eng 38:57–61
18. Florian JA, Parker RS (2005) Empirical modeling for glucose control in diabetes and critical care. Eur J Control 11:605–616
19. Freckmann G, Kalatz B, Pfeiffer B, Hoss U, Haug C (2001) Recent advances in continuous glucose monitoring. Exp Clin Endocrinol Diab 109(Suppl 2):S347–S357
20. Furler SM, Kraegen EW, Smallwood RH, Chisolm DJ (1985) Blood glucose control by intermittent loop closure in the basal model: computer simulation studies with a diabetic model. Diab Care 8:553–561
21. Ginsberg J (2007) The current environment of CGM technologies. J. Diab Sci Technol 1:111–127
22. Godsland IF, Agbaje OF, Hovorka R (2006) Evaluation of nonlinear regression approaches to estimation of insulin sensitivity by the minimal model with reference to Bayesian hierarchical analysis. Am J Physiol Endocrinol Metab 291:E167–E174
23. Krudys KM, Kahn SE, Vicini P (2006) Population approaches to estimate minimal model indexes of insulin sensitivity and glucose effectiveness using full and reduced sampling schedules. Am J Physiol Endocrinol Metab 291:E716–E723
24. Lefebvre PJ, Paolisso G, Sheen AJ, Henquin JC (1987) Pulsatility of insulin and glucagon release: physiological significance and pharmacological implications. Diabetologia 30:443–452
25. Lynch SM, Bequette BW (2002) Model predictive control of blood glucose in Type 1 diabetics using subcutaneous glucose measurements. In: Proceedings of American control conference, Anchorage, AK, pp 4039–4043
26. Markakis MG, Mitsis GD, Marmarelis VZ (2008) Computational study of an augmented minimal model for glycaemia control. In: Proceedings of the 30th annual IEEE-EMBS conference, Vancouver, BC, Canada, pp 5445–5448
27. Markakis, M.G., Mitsis, G.D., Papavassilopoulos, G.P., Marmarelis, V.Z.: Model Predictive Control of Blood Glucose in Type 1 Diabetics: the Principal Dynamic Modes Approach. Proc. 30th Annual IEEE-EMBS Conf., Vancouver, BC, Canada, 5466-5469 2008

28. Marmarelis VZ (1991) Wiener analysis of nonlinear feedback in sensory systems. Ann Biomed Eng 19:345–382
29. Marmarelis VZ (1997) Modeling methodology for nonlinear physiological systems. Ann Biomed Eng 25:239–251
30. Marmarelis VZ (2004) Nonlinear dynamic modeling of physiological systems. IEEE-Wiley, Piscataway
31. Mitsis GD, Marmarelis VZ (2002) Modeling of nonlinear physiological systems with fast and slow dynamics. I. Methodology. Ann Biomed Eng 30:272–281
32. Mitsis GD (2002) Nonlinear physiological system modeling with Laguerre-Volterra networks: methods and applications. Ph.D. thesis, Department of Biomedical Engineering, University of Southern California
33. Muniyappa R, Lee S, Chen H, Quon MJ (2008) Current approaches for assessing insulin sensitivity and resistance in vivo: advantages, limitations, and appropriate usage. Am J Physiol Endocrinol Metab 294(1):E15–E26
34. Ni TC, Ader M, Bergman RN (1997) Reassessment of glucose effectiveness and insulin sensitivity from minimal model analysis: a theoretical evaluation of the single-compartment glucose distribution assumption. Diabetes 46:1813–1821
35. Parker RS, Doyle FJ, 3rd Peppas NA (1999) A model-based algorithm for blood glucose control in type I diabetic patients. IEEE Trans Biomed Eng 46:148–157
36. Porksen N (2002) The in vivo regulation of pulsatile insulin secretion. Diabetologia 45:3–20
37. Roy A, Parker RS (2006) Dynamic modeling of free fatty acid, glucose, and insulin: an extended "minimal model". Diab Technol Ther 8:617–626
38. Sorensen J (1985) A physiologic model of glucose metabolism in man and its use to design and assess insulin therapies for diabetes. Ph.D. thesis, Department of Chemical Engineering, Massachussetts Institute of Technology, Cambridge, MA
39. Steil GM, Rebrin K, Janowski R, Darwin C, Saad MF (2003) Modeling beta-cell insulin secretion-implications for closed-loop glucose homeostasis. Diab Technol Ther 5:953–964
40. Sturis J, Van Cauter EV, Blackman JD, Polonsky KS (1991) Entrainment of pulsatile insulin secretion by oscillatory glucose infusion. J Clin Invest 87:439–445
41. Toffolo G, Bergman RN, Finegood DT, Bowden CR, Cobelli C (1980) Quantitative estimation of beta cell sensitivity to glucose in the intact organism: a minimal model of insulin kinetics in the dog. Diabetes 29:979–990
42. Toffolo G, Campioni M, Basu R, Rizza RA, Cobelli C (2006) A minimal model of insulin secretion and kinetics to assess hepatic insulin extraction. Am J Physiol Endocrinol Metab 290:E169–E176
43. Tresp V, Briegel T, Moody J (1999) Neural-network models for the blood glucose metabolism of a diabetic. IEEE Trans Neur Netw 10:1204–1213
44. Van Cauter EV, Shapiro ET, Tillil H, Polonsky KS (1992) Circadian modulation of glucose and insulin responses to meals-relationship to cortisol rhythm. Am J Physiol 262:R467–R475
45. Van Herpe T, Pluymers B, Espinoza M, Van den Berghe G, De Moor B (2006) A minimal model for glycemia control in critically ill patients. In: Proceedings of the 28th IEEE EMBS annual international conference, New York, NY